

Journal of Biomedical Optics

SPIEDigitalLibrary.org/jbo

Birefringence of the central cornea in children assessed with scanning laser polarimetry

Kristina Irsch
Ashesh A. Shah

Birefringence of the central cornea in children assessed with scanning laser polarimetry

Kristina Irsch^a and Ashesh A. Shah^b

^aJohns Hopkins University School of Medicine, Wilmer Eye Institute, Baltimore, Maryland

^bUniversity of Heidelberg, Medical Physics, Heidelberg, Germany

Abstract. Corneal birefringence is a well-known confounding factor with all polarization-sensitive technology used for retinal scanning and other intraocular assessment. It has been studied extensively in adults, but little is known regarding age-related differences. Specifically, no information is available concerning corneal birefringence in children. For applications that are geared towards children, such as retinal birefringence scanning for strabismus screening purposes, it is important to know the expected range of both corneal retardance and azimuth in pediatric populations. This study investigated central corneal birefringence in children (ages three and above), by means of scanning laser polarimetry (GDx-VCC™, Carl Zeiss Meditec, Inc.). Children's measures of corneal retardance and azimuth were compared with those obtained in adults. As with previous studies in adults, corneal birefringence was found to vary widely in children, with corneal retardance ranging from 10 to 77 nm, and azimuth (slow axis) ranging from -11° to 71° (measured nasally downward). No significant differences in central corneal birefringence were found between children and adults, nor were significant age-related differences found in general. In conclusion, establishing knowledge of the polarization properties of the central cornea in children allows better understanding, exploitation, or bypassing of these effects in new polarization-sensitive pediatric ophthalmic applications.

© 2012 Society of Photo-Optical Instrumentation Engineers (SPIE). [DOI: 10.1117/1.JBO.17.8.086001]

Keywords: polarization-sensitive ophthalmic technology; ophthalmology; retina; imaging; cornea; birefringence; polarimetry; polarized light.

Paper 12255 received Apr. 26, 2012; revised manuscript received Jun. 30, 2012; accepted for publication Jul. 3, 2012; published online Aug. 6, 2012.

1 Introduction

Polarization-sensitive ophthalmic technologies, such as scanning laser polarimetry,^{1,2} polarization-sensitive optical coherence tomography,³⁻⁵ retinal birefringence scanning (RBS),⁶⁻⁹ polarimetric blood glucose sensing,^{10,11} are known to be adversely affected by corneal birefringence.^{5,12-19} Although being relatively constant over the central area for any given eye,²⁰ corneal birefringence varies widely among individuals and eyes in both its amount (corneal retardance) and orientation (corneal azimuth).^{21,22} Since light must pass through this major birefringent ocular medium before reaching the retina or any other polarization-sensitive structure of interest within the eye, polarization-related changes caused by the cornea must be dealt with.

Corneal birefringence has been studied extensively in adults,²¹⁻²⁴ and various methods have been proposed to factor out or compensate for it,^{2,12-15,25,26} generally involving a separate measurement and feedback system. However, little is known regarding age-related differences.^{22,27} Specifically, to the best of the authors' knowledge, no information is available concerning corneal birefringence in children.

For technology that is also applicable to children,²⁸⁻³² in particular for applications that are geared towards children such as RBS for strabismus screening purposes,^{8,9,16} where methods of bypassing corneal birefringence rather than individual compensation are desired,¹⁸ knowledge of the expected

range of corneal retardance and azimuth in pediatric populations is essential to understand and allow development of optimal approaches to bypass interference from these variable optical properties.

The purpose of this study was to establish knowledge of the polarization properties of the central corneas in a pediatric population, and compare children's measures of corneal retardance and azimuth with those obtained in adults.

2 Polarization Properties of the Central Cornea

To understand possible changes of corneal birefringence with age, one must first understand the origin of this birefringence. The cornea is not only the major refractive component of the eye, but it also contributes most to the overall ocular birefringence. The human cornea is composed of five different layers, starting from anterior to posterior: the epithelium, Bowman's layer, the stroma, Descemet's membrane, and the endothelium. Its main constituent is the corneal stroma, which makes up 90% of the entire thickness, and is also responsible for its birefringence. In the central cornea, the stroma is composed of approximately 200-300 lamellae,³³ lying parallel to the corneal surface.³⁴ Each of the corneal lamellae contains collagen fibrils, closely packed fibers embedded in an optically homogeneous ground substance.³⁵ The collagen fibers within individual lamellae are parallel, but they have different orientations with adjacent lamellae that are stacked on top of one another.^{34,36}

Corneal birefringence is a combination of intrinsic and form birefringence. Intrinsic birefringence has its origin in the optical anisotropy within the collagen fibers,^{35,37} which are composed

Address all correspondence to: Kristina Irsch, Johns Hopkins University School of Medicine, The Wilmer Eye Institute, Baltimore, Maryland. Tel: (443) 287-0068; Fax: (410) 955-0809; E-mail: kirsch1@jhmi.edu

predominately of type I collagen molecules that are known to exhibit positive uniaxial birefringence.³⁸ The ordered arrangement of the fibers within individual lamellae, embedded in an isotropic ground substance of different refractive index, produces corneal “form” birefringence,³⁷ and accounts for more than two-thirds of the total corneal birefringence.³⁸ Each lamella may be considered as a birefringent plate or linear retarder with its axis of birefringence (slow axis) lying along the direction of the collagen fibers, leading to the simplified consideration of the corneal stroma as a series of stacked birefringent plates, with their slow axes lying at various angles to one another.^{33,39} A slight prevalence of one lamella orientation results in a net amount and axis of birefringence.

3 Central Cornea During Development

Developmental and age-related changes in the structure of the central cornea, and in particular changes in the structure and thickness of the stroma, are critical to the understanding of the optical behavior of central corneal birefringence with development and aging.

Overall central corneal thickness increases during gestation,⁴⁰ and then decreases after birth, from values found in premature^{41,42} and full-term newborns^{43–48} to those found in small children from 2 years of age.^{43,47} Only little or no further change in central corneal thickness is expected thereafter.^{49,50} This is in agreement with Lagrèze’s results showing that corneal diameter reaches a plateau at approximately two years of age.⁵¹ Decrease in central corneal thickness is associated with increase of corneal diameter occurring with the general growth of the eye.⁴² The most rapid decrease in central corneal thickness occurs in the first days^{45,46} and early months of life, when corneal diameter grows fastest,⁵² and then abruptly slows during early childhood. Hymes concluded that the cornea reaches its mean adult size in the period between six months and one year of life.⁵³

The stroma, in particular, as being responsible for corneal birefringence, increases in thickness from 229 μm at 20 weeks of gestation to 490 μm at six months after birth, at which time the adult thickness (500 μm) has essentially been reached.⁴⁰ The collagen lamellae, that are known to be oriented differently in the anterior and posterior part of the stroma, are more vertically oriented in the anterior part in early stages of development. The collagen fibrils, which combine to form the lamellae, are parallel to each other in the same lamellae irrespective of age and location of the lamellae, with their periodic structure already being observed at 20 weeks of gestation. According to Kanai and Kaufmann, the lamellae begin to add to their individual thickness, not to their number, when the cornea has reached one quarter of its adult thickness.⁵⁴ The gap between the lamellae is about 16 nm, and remains unchanged during the developmental process. The diameter of the collagen fibrils, however, increases slightly, from 25 nm (20 weeks of gestation) to 33.3 nm (six months after birth),⁴⁰ which in turn results in an increase in thickness of collagen lamellae from between 0.5 to 1 μm (20 weeks of gestation) to between 1.5 to 2 μm (six months after birth). The collagen lamellae in an adult corneal stroma have a thickness between 2 to 6 μm ,⁴⁰ and collagen fibers have an average diameter between 25 and 30 nm.⁵⁴

Small structural changes continue to occur with aging.⁵⁵ For example, the diameter of collagen fibrils increases, which appears mostly to be due to an increased number of collagen

molecules within the fibrils of elderly individuals, and to an expansion of the intermolecular spacing of the collagen fibrils.⁵⁶ Further, the cross-sectional area associated with each molecule in corneal collagen increases with age. Over a 90-year time span, there is, on average, an increase in cross-sectional area from approximately 3.04 to 3.46 nm^2 .⁵⁷ In contrast, there is a decrease in the interfibrillary distance with age, in accordance with Kanai and Kaufmann,⁵⁴ who also observed a greater breakdown of fibers, along with multiple small collagen-free spaces.

4 Methods

Corneal birefringence was measured with the help of a GDx-VCC instrument (Carl Zeiss Meditec, Inc.), as described previously.¹⁸ The GDx is a commercially available scanning laser polarimeter primarily used for glaucoma diagnostic purposes. It makes use of the linear relationship between the thickness of a birefringent medium and its retardation.⁵⁸ By measuring the total retardation of the birefringent retinal nerve fiber layer point by point in a raster pattern, from the change in polarization state in the light retroreflected from the fundus of the eye, a “topographic map” of the nerve fiber thickness in the eye’s retina can be created, providing a quantitative method for detecting eye diseases such as glaucoma, which is characterized by loss of nerve fibers in its early state.^{2,59,60} The variable corneal compensator (VCC) version of the instrument features two identical wave plates in rotary mounts that allow measurement and individual neutralization of corneal birefringence.^{12,13}

Corneal birefringence is measured with the magnitude of the VCC set to zero, accomplished by simply rotating both retarders such that their fast axes are perpendicular to each other. Polarimetry images of a normal macula, with no ocular disease, obtained in this “crossed” position demonstrates a non-uniform retardation map with a distinct “bow-tie” pattern about the fovea, representing the retardation of the cornea superimposed onto the retardation of the radially symmetric birefringent Henle fibers about the fovea, from whose orientation the azimuth of the corneal birefringence can be obtained directly. Corneal retardance is determined from the retardation profile around a ~ 1.41 mm diameter circle centered on the fovea¹² (about 4.7 deg in visual angle).

Ninety-one subjects, including 47 children (ages three and above) and 48 adults (ages 18 and above), who had no history of corneal or retinal disease, and who had not undergone refractive or cataract surgery, participated in this study, which was approved by The Johns Hopkins University Institutional Review Board and followed the tenets of the Declaration of Helsinki. Prior to the investigations, informed consent was obtained from either the subject or the parent after the nature and possible consequences of the research study were explained. Single-pass corneal retardance and corneal azimuth (measured downward from nasally) were measured in both eyes of the 91 subjects. Only those measurements with a GDx quality score of eight (out of 10) and above were included in the analysis. Therefore, for some subjects only one eye was taken into account for the analysis.

Statistical analysis was performed using commercially available software (SAS, Matlab, Excel). The Shapiro-Wilk test was used to check whether the data were normally distributed (p -value; $P > 0.05$) or not normally distributed ($P < 0.05$) and to decide whether parametric or non-parametric statistical

test procedures should be used. For normally distributed data, independent *t*-tests were used to compare mean differences of corneal retardance and corneal azimuth between the eyes, while paired *t*-tests were used to compare mean differences between paired eyes. For non-normally distributed data, the Wilcoxon rank-sum test was used to compare median differences of corneal retardance and corneal azimuth between the eyes, and between children and adults (because children and adult eyes combined were not normally distributed), while the Wilcoxon signed-rank test was used to compare median differences between paired eyes. A *p*-value (*P*) of less than 0.05 was considered statistically significant. Correlations were calculated with Pearson's correlation coefficient (*r*) and Spearman's correlation coefficient (ρ) for normally and non-normally distributed data, respectively. The relationship of subject age with corneal birefringence was assessed using generalized linear regression and generalized estimating equations (GEE) models.

5 Results

The corneal retardance in the eyes of the 47 children ranged from 10 to 77 nm (mean \pm SD = 39 nm \pm 16 nm), and corneal azimuth ranged from -11° to 71° (mean \pm SD = $23^\circ \pm 17^\circ$). Corneal birefringence was normally distributed in both eyes (Shapiro-Wilk test; *P* = 0.36 for corneal retardance and *P* = 0.35 for corneal azimuth). The distributions of corneal retardances and corneal azimuths are depicted graphically using histograms in Fig. 1, and box plots in Fig. 2.

Corneal birefringence was highly correlated between left and right eyes; *r* = 0.81 for corneal retardance and *r* = 0.79 for corneal azimuth (*P* < 0.0001). Corneal retardance was not correlated with corneal azimuth for either eye; *r* = -0.03 (*P* = 0.86) for left eye and *r* = -0.03 (*P* = 0.87) for right eye. While no significant difference was found for corneal azimuth between eyes [Fig. 2(a); *P* = 1.00 between all left and right eyes and *P* = 0.32 between paired eyes], left eye corneal

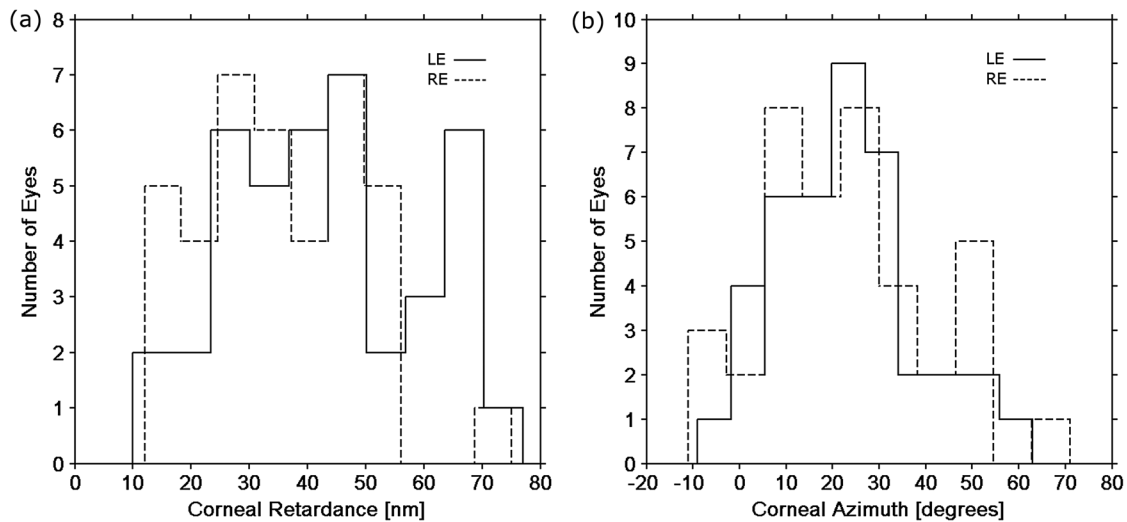


Fig. 1 Distributions of corneal retardances (a) and corneal azimuths (b) in right eyes (RE, dashed line) and left eyes (LE, solid line) of 47 children. Postive corneal azimuth values are nasally downward.

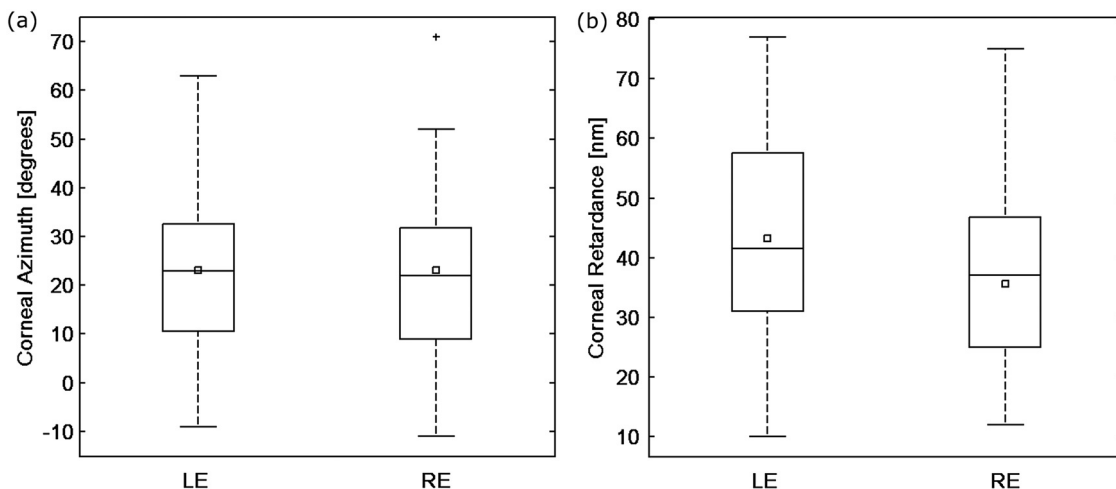


Fig. 2 Box plot representation of corneal azimuths (a) and corneal retardances (b) between the left eyes (LE) and right eyes (RE). The median is identified by the horizontal line within the box. The length of the box represents the interquartile range (IQR), with the edges being the 25th (lower quartile) and 75th (upper quartile) percentiles. The ends of the whiskers represent minimum and maximum values. Values more than 1.5 IQRs are labeled as outliers (+). In addition, the mean is shown as square.

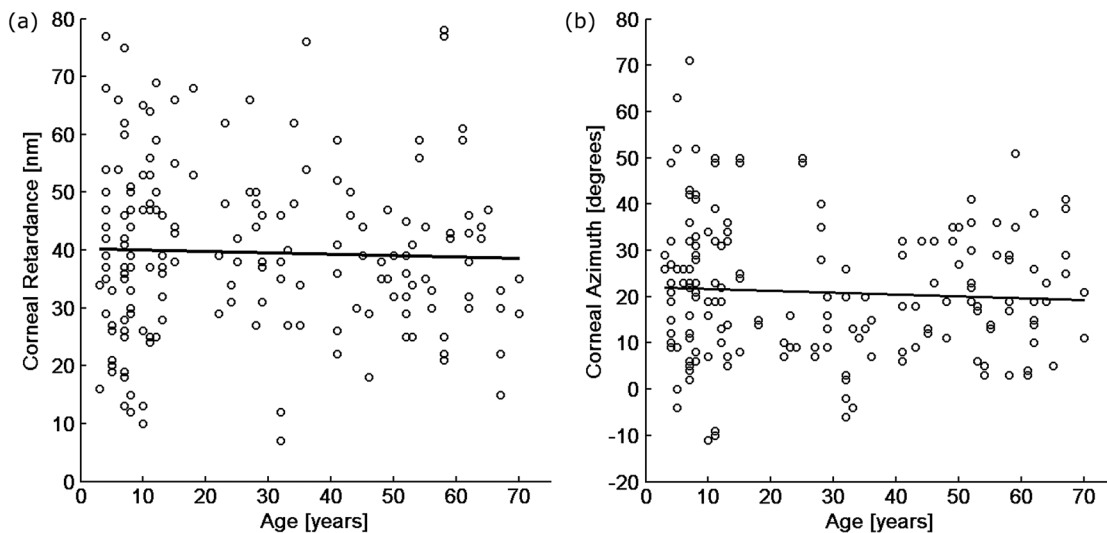


Fig. 3 Scatter plot showing relationship of age with corneal retardance (a) and corneal azimuth (b). The lines are from a generalized linear regression analysis.

retardance was significantly greater than right eye corneal retardance [Fig. 2(b); $P = 0.03$ between all left and right eyes and $P = 0.0001$ between paired eyes, i.e. less than 0.05 significance level].

Corneal retardance and azimuth were measured in the 48 adults to allow assessment of differences between child and adult measures, as well as age-related differences. Adult measures of corneal retardance ranged from 7 to 78 nm (mean \pm SD = 39 nm \pm 14 nm), and corneal azimuth ranged from -6° to 51° (mean \pm SD = $19^\circ \pm 13^\circ$).

Unlike with children, adult measures of corneal birefringence were not normally distributed; the distribution of corneal retardances was close to normal (Shapiro-Wilk test; $P = 0.05$ for corneal retardance and $P = 0.04$ for corneal azimuth). As with children, corneal birefringence was highly correlated between left and right eyes; $\rho = 0.73$ for corneal retardance and $\rho = 0.84$ for corneal azimuth ($P < 0.0001$). While corneal retardance was not correlated with corneal azimuth for right eyes ($\rho = -0.08$, $P = 0.62$), a low correlation between corneal retardance and corneal azimuth was found in left eyes ($\rho = -0.30$, $P = 0.04$), in that weaker corneal retardance was associated with more nasally downward corneal azimuths. As with children, no significant difference was found for corneal azimuth between eyes ($P = 0.95$ between paired eyes and $P = 0.93$ between all left and right eyes), whereas left eye corneal retardance was significantly greater than right eye corneal retardance between paired eyes ($P = 0.01$), and marginally significant between all left and right eyes ($P = 0.07$).

No significant differences in central corneal birefringence were found between children and adults, either with the Wilcoxon rank-sum test or with GEE which were used to take the correlation between two eyes for the same subject into account: P (Wilcoxon rank-sum test) = 0.96 and P (GEE model) = 0.98 for corneal retardance; and P (Wilcoxon rank-sum test) = 0.12 and P (GEE model) = 0.15 for corneal azimuth. Further generalized linear regression analysis [Fig. 3(a): $R^2 = 0.001$, slope = -0.02 , $P = 0.65$ for corneal retardance and Fig. 3(b): $R^2 = 0.003$, slope = -0.04 , $P = 0.45$ for corneal retardance] and GEE (slope = -0.03 , $P = 0.70$ for corneal retardance and slope = -0.05 , $P = 0.42$ for corneal azimuth) showed no

significant relationship between central corneal birefringence and continuous age.

6 Discussion and Conclusion

In accordance with previous studies in adults,^{21–23} our results in children show that corneal birefringence varies widely in both its amount and orientation from one eye to the next.

Our results in adults are similar to those previously reported.^{21,22} In our study, however, the distribution of adult eyes was not normal (close to normal for corneal retardance; $P = 0.05$). Similar to Knighton and Huang²¹ who found a correlation between corneal retardance and corneal azimuth ($r = 0.37$ for left eyes and $r = 0.59$ for right eyes; $P < 0.002$), in that weaker corneal retardance was associated with more nasally downward corneal azimuths, we observed this relationship in left eyes ($\rho = -0.30$, $P = 0.04$) but not in right eyes ($\rho = -0.08$, $P = 0.62$) in our study.

Statistical analysis suggests that there is no significant difference in either corneal retardance or azimuth between children (ages three and above) and adults, and no significant age-related differences in general.

This is in accord with the literature available on structural changes of the central cornea with development and aging. Although substantial changes in central corneal thickness occur in infancy and in very early childhood, the structure of the central cornea, and in particular the structure and thickness of the stroma, which give rise to corneal birefringence from the lamellar-arranged collagen fibers, essentially reach adult values at about six months after birth,⁴⁰ with only small structural changes occurring thereafter.⁵⁶

This explains why no significant differences in central corneal birefringence were observed between children and adults. We did, however, find a significant difference between right and left eye corneal retardance, in that the left eye corneal retardance was significantly greater than that of the right eye. Levy, et al., were first to report such an intraocular difference in adults,⁶¹ and attributed this difference in retardance as being an artifact due to the inherent asymmetry between right and left eye measurement with the GDx-VCC, resulting in a more nasal measurement of corneal retardance in the left eye where the Henle fiber layer

appears to be thicker^{62,63} and a more temporal measurement in the right eye.

In conclusion, this study, for the first time, investigated the birefringence of the central cornea in children. Our results suggest that there are no significant differences in central corneal birefringence between children and adults, in accord with available literature on developmental and age-related changes of the central cornea. Expanding our knowledge of the polarization properties of the central cornea to a larger range of the population, including children, allows better understanding, exploitation, or bypassing of these effects in new polarization-sensitive ophthalmic technology.

Acknowledgments

This study was partly supported by the Hartwell Foundation and by gifts from Robert and Maureen Feduniak, Dewey and Janet Gargiulo, David and Helen Leighton, Richard and Victoria Baks, and Robert and Diane Levy. The authors thank Boris Gramatikov, PhD, for encouragement to undertake this study, David Guyton, MD, for proofreading the manuscript, and Carl Zeiss Meditec for providing assistance with the GDx-VCC manuals and a software update. The authors further thank David Guyton, MD, Hee-Jung Park, MD, Anya Trumler, MD, Alex Christoff, Xiaonong Liu, Rita Dziecichowicz, and Mike Piorunski for helping with the recruitment of subjects for the study. The authors also want to gratefully acknowledge Jing Tian, MS, from the Wilmer Biostatistical Center, for her assistance in statistical analysis and consultation.

References

1. A. W. Dreher and K. Reiter, "Scanning laser polarimetry of the retinal nerve fiber layer," *Proc. SPIE* **1746**, 34–41 (1992).
2. A. W. Dreher and K. Reiter, "Retinal eye disease diagnostic system," U. S. Patent No. 5,303,709 (1994).
3. M. R. Hee et al., "Polarization-sensitive low-coherence reflectometer for birefringence characterization and ranging," *J. Opt. Soc. Am. B* **9**(6), 903–908 (1992).
4. E. Götzinger, M. Pircher, and C. K. Hitzenberger, "High speed spectral domain polarization sensitive optical coherence tomography of the human retina," *Opt. Express* **13**(25), 10217–10229 (2005).
5. M. Pircher et al., "Corneal birefringence compensation for polarization sensitive optical coherence tomography of the human retina," *J. Biomed. Opt.* **12**(4), 041210 (2007).
6. D. G. Hunter, S. N. Patel, and D. L. Guyton, "Automated detection of foveal fixation by use of retinal birefringence scanning," *Appl. Opt.* **38**(7), 1273–1279 (1999).
7. D. L. Guyton et al., "Eye fixation monitor and tracker," U. S. Patent No. 6,027,216 (2000).
8. D. G. Hunter et al., "Automated detection of ocular alignment with binocular retinal birefringence scanning," *Appl. Opt.* **42**(16), 3047–3053 (2003).
9. D. G. Hunter et al., "Pediatric Vision Screener 1: instrument design and operation," *J. Biomed. Opt.* **9**(6), 1363–1368 (2004).
10. S. Kozaitis et al., "Laser polarimetry for measurement of drugs in the aqueous humor," in *Proc. IEEE*, Vol. **13**, pp. 1570–1571 (1991).
11. T. W. King et al., "Multispectral polarimetric glucose detection using a single Pockels cell," *Opt. Eng.* **33**(8), 2746–2753 (1994).
12. Q. Zhou and R. N. Weinreb, "Individualized compensation of anterior segment birefringence during scanning laser polarimetry," *Invest. Ophthalmol. Vis. Sci.* **43**(7), 2221–2228 (2002).
13. Q. Zhou, "System and method for determining birefringence of anterior segment of the patient's eye," U. S. Patent No. 6,356,036 (2002).
14. Q. Zhou, "Retinal scanning laser polarimetry and methods to compensate for corneal birefringence," *Bull. Soc. Belge Ophthalmol.* **302**, 89–106 (2006).
15. N. J. Reus, Q. Zhou, and H. G. Lemij, "Enhanced imaging algorithm for scanning laser polarimetry with variable corneal compensation," *Invest. Ophthalmol. Vis. Sci.* **47**(9), 3870–3877 (2006).
16. K. Irsch, "Polarization modulation using wave plates to enhance foveal fixation detection in retinal birefringence scanning for pediatric vision screening purposes," Ph.D. thesis, University of Heidelberg, Germany (2009), <http://www.ub.uni-heidelberg.de/archiv/8938/>.
17. K. Irsch et al., "Spinning wave plate design for retinal birefringence scanning," *Proc. SPIE* **7169**, 71691F (2009).
18. K. Irsch et al., "Modeling and minimizing interference from corneal birefringence in retinal birefringence scanning for foveal fixation detection," *Biomed. Opt. Express* **2**(7), 1955–1968 (2011).
19. B. H. Malik and G. L. Coté, "Modeling the corneal birefringence of the eye toward the development of a polarimetric glucose sensor," *J. Biomed. Opt.* **15**(3), 037012 (2010).
20. G. J. Van Blokland and S. C. Verhelst, "Corneal polarization in the living human eye explained with a biaxial model," *J. Opt. Soc. Am. A* **4**(1), 82–90 (1987).
21. R. W. Knighton and X. R. Huang, "Linear birefringence of the central human cornea," *Invest. Ophthalmol. Vis. Sci.* **43**(1), 82–86 (2002).
22. R. N. Weinreb et al., "Measurement of the magnitude and axis of corneal polarization with scanning laser polarimetry," *Arch. Ophthalmol.* **120**(7), 901–906 (2002).
23. D. S. Greenfield, R. W. Knighton, and X. R. Huang, "Effect of corneal polarization axis on assessment of retinal nerve fiber layer thickness by scanning laser polarimetry," *Am. J. Ophthalmol.* **129**(6), 715–722 (2000).
24. R. W. Knighton, X. R. Huang, and L. A. Cavuoto, "Corneal birefringence mapped by scanning laser polarimetry," *Opt. Express* **16**(18), 13738–13751 (2008).
25. B. C. E. Pelz et al., "In vivo measurement of the retinal birefringence with regard on corneal effects using an electro-optical ellipsometer," *Proc. SPIE* **2930**, 92–101 (1996).
26. R. W. Knighton and X. R. Huang, "Analytical methods for scanning laser polarimetry," *Opt. Express* **10**(21), 1179–1189 (2002).
27. T. A. Mai and H. G. Lemij, "Longitudinal measurement variability of corneal birefringence and retinal nerve fiber layer thickness in scanning laser polarimetry with variable corneal compensation," *Arch. Ophthalmol.* **126**(10), 1359–1364 (2008).
28. D. B. Hess et al., "Macular and retinal nerve fiber layer analysis of normal and glaucomatous eyes in children using optical coherence tomography," *Am. J. Ophthalmol.* **139**(3), 509–517 (2005).
29. D. J. Salchow and K. A. Hutcheson, "Optical coherence tomography applications in pediatric ophthalmology," *J. Pediatr. Ophthalmol. Strabismus* **44**(6), 335–349 (2007).
30. M. A. El-Dairi et al., "Optical coherence tomography in the eyes of normal children," *Arch. Ophthalmol.* **127**(1), 50–58 (2009).
31. C. Gerth et al., "High-resolution retinal imaging in young children using a handheld scanner and Fourier-domain optical coherence tomography," *J. AAPOS* **13**(1), 72–74 (2009).
32. R. S. Maldonado et al., "Optimizing hand-held spectral domain optical coherence tomography imaging for neonates, infants, and children," *Invest. Ophthalmol. Vis. Sci.* **51**(5), 2678–2685 (2010).
33. R. A. Farrell, D. Rouseff, and R. L. McCally, "Propagation of polarized light through two- and three-layer anisotropic stacks," *J. Opt. Soc. Am. A* **22**(9), 1981–1992 (2005).
34. K. M. Meek and C. Boote, "The use of X-ray scattering techniques to quantify the orientation and distribution of collagen in the corneal stroma," *Prog. Retin. Eye Res.* **28**(5), 369–392 (2009).
35. D. M. Maurice, "The structure and transparency of the cornea," *J. Physiol.* **136**(2), 263–286 (1957).
36. K. M. Meek and C. Boote, "The organization of collagen in the corneal stroma," *Exp. Eye Res.* **78**(3), 503–512 (2004).
37. L. J. Bour, "Polarized light and the eye," Chap. 13, in *Visual Optics and Instrumentation*, W. N. Charman, ed., Macmillan Press, New York, NY, pp. 310–325 (1991).
38. G. P. Misson, "The theory and implications of the biaxial model of corneal birefringence," *Ophthalm. Physiol. Opt.* **30**(6), 834–846 (2010).
39. D. J. Donohue et al., "Numerical modeling of the cornea's lamellar structure and birefringence properties," *J. Opt. Soc. Am. A* **12**(7), 1425–1438 (1995).

40. L. Lesueur et al., "Structural and ultrastructural changes in the developmental process of premature infants' and children's corneas," *Cornea* **13**(4), 331–338 (1994).
41. T. Autzen and L. Bjørnstrøm, "Central corneal thickness in premature babies," *Acta Ophthalmol. (Copenh.)* **69**(2), 251–252 (1991).
42. C. Kirwan, M. O'Keefe, and S. Fitzsimon, "Central corneal thickness and corneal diameter in premature infants," *Acta Ophthalmol. Scand.* **83**(6), 751–753 (2005).
43. N. Ehlers et al., "Central corneal thickness in newborns and children," *Acta Ophthalmol. (Copenh.)* **54**(3), 285–290 (1976).
44. T. Autzen and L. Bjørnstrøm, "Central corneal thickness in full-term newborns," *Acta Ophthalmol. (Copenh.)* **67**(6), 719–720 (1989).
45. W. Portellinha and R. Belfort, "Central and peripheral corneal thickness in newborns," *Acta Ophthalmol. (Copenh.)* **69**(2), 247–250 (1991).
46. L. Remón et al., "Central and peripheral corneal thickness in full-term newborns by ultrasonic pachymetry," *Invest. Ophthalmol. Vis. Sci.* **33**(11), 3080–3083 (1992).
47. H. U. Møller, "Milestones and normative data," Chap. 5, in *Pediatric ophthalmology and strabismus*, D. Taylor and C. S. Hoyt, eds., Elsevier Saunders, Philadelphia, PA, p. 36 (2005).
48. M. G. Uva et al., "Intraocular pressure and central corneal thickness in premature and full-term newborns," *J. AAPOS* **15**(4), 367–369 (2011).
49. M. J. Doughty and M. L. Zaman, "Human corneal thickness and its impact on intraocular pressure measures: a review and meta-analysis approach," *Surv. Ophthalmol.* **44**(5), 367–408 (2000).
50. S. Jonuscheit and M. J. Doughty, "Evidence for a relative thinning of the peripheral cornea with age in white European subjects," *Invest. Ophthalmol. Vis. Sci.* **50**(9), 4121–4128 (2009).
51. W. A. Lagrèze and G. Zobor, "A method for noncontact measurement of corneal diameter in children," *Am. J. Ophthalmol.* **144**(1), 141–142 (2007).
52. A. Ronneburger, J. Basarab, and H. C. Howland, "Growth of the cornea from infancy to adolescence," *Ophthalm. Physiol. Opt.* **26**(1), 80–87 (2006).
53. C. Hymes, "The postnatal growth of the cornea and palpebral fissure and the projection of the eyeball in early life," *J. Comp. Neurol.* **48**(3), 415–440 (1929).
54. A. Kanai and H. E. Kaufman, "Electron microscopic studies of corneal stroma: aging changes of collagen fibers," *Ann. Ophthalmol.* **5**(3), 285–287 (1973).
55. K. B. Gunton, L. B. Nelson, and S. E. Olitsky, "Neonatal Ophthalmology: Ocular development in childhood" Chap. 2, in *Harley's pediatric ophthalmology*, R. D. Harley, L. B. Nelson, and S. E. Olitsky, eds., Lippincott Williams & Wilkins, Philadelphia, PA, pp. 53–66 (2005).
56. A. Daxer et al., "Collagen fibrils in the human corneal stroma: structure and aging," *Invest. Ophthalmol. Vis. Sci.* **39**(3), 644–648 (1998).
57. N. S. Malik et al., "Ageing of the human corneal stroma: structural and biochemical changes," *Biochim. Biophys. Acta.* **1138**(3), 222–228 (1992).
58. O. Wiener, "Die Theorie des Mischkörpers für das Feld der Stationären Strömung," *Abh. Sachs. Ges. Akad. Wiss. Math. Phys. Kl.* **32**(6), 507–604 (1912).
59. R. N. Weinreb et al., "Histopathologic validation of Fourier-ellipsometry measurements of retinal nerve fiber layer thickness," *Arch. Ophthalmol.* **108**(4), 558–560 (1990).
60. R. N. Weinreb, S. Shakiba, and L. Zangwill, "Scanning laser polarimetry to measure the nerve fiber layer of normal and glaucomatous eyes," *Am. J. Ophthalmol.* **119**(5), 626–636 (1995).
61. N. S. Levi and I. H. Schachar, "Accuracy of GDx variable corneal compensation polarization measurements in human eyes: effect of accommodation, cycloplegia, focus, pupil size, and eye selection on reproducibility," *Eye (Lond.)* **21**(3), 333–340 (2007).
62. R. Varma, M. Skaf, and E. Barron, "Retinal nerve fiber layer thickness in normal human eyes," *Ophthalmology* **103**(12), 2114–2119 (1996).
63. M. Shahidi, Z. Wang, and R. Zelkha, "Quantitative thickness measurement of retinal layers imaged by optical coherence tomography," *Am. J. Ophthalmol.* **139**(6), 1056–1061 (2005).